J. Austral. Math. Soc. Ser. B 26 (1984), 14–30

AN INTEGRAL EQUATION FOR IMMISCIBLE FLUID DISPLACEMENT IN A TWO-DIMENSIONAL POROUS MEDIUM OR HELE-SHAW CELL

M. R. DAVIDSON[1]

(Received 29 September 1982; revised 18 March 1983)

Abstract

An integral equation for the normal velocity of the interface between two immiscible fluids flowing in a two-dimensional porous medium or Hele-Shaw cell (one fluid displaces the other) is derived in terms of the physical parameters (including interfacial tension), a Green's function and the given interface. When the displacement is unstable, 'fingering' of the interface occurs. The Saffman-Taylor interface solutions for the steady advance of a single parallel-sided finger in the absence of interfacial tension are seen to satisfy the integral equation, and the error incurred in that equation by the corresponding Pitts approximating profile, when interfacial tension is included, is shown. In addition, the numerical solution of the integral equation is illustrated for a sinusoidal and a semicircular interface and, in each case, the amplitude behaviour inferred from the velocity distribution is consistent with conclusions based on the stability of an initially flat interface.

1. Introduction

When the displacement of one fluid by another in a porous medium is unstable, it is characterised by the development of long fingers of displacing fluid which penetrate the displaced fluid region. This phenomenon is of particular interest in the oil industry where it reduces the efficiency of oil recovery (e.g. during water or gas drive). Other fields in which the phenomenon may be encountered include groundwater hydrology (saltwater-freshwater interface in coastal aquifers) and soil sciences (infiltration flows).

[1]CSIRO Division of Mineral Physics, Lucas Heights Research Laboratories, Private Mail Bag 7, Sutherland, N.S.W. 2232.

Fingering can occur, for example, when the flow is directed from a less viscous to a more viscous fluid, provided that the velocity is large enough. In laboratory studies of this phenomenon carried out in linear Hele-Shaw models (the thickness averaged flow equations for a Hele-Shaw cell are mathematically analogous to two-dimensional flow in a porous medium) it is observed that, following the formation of a number of fingers, one of them tends to dominate, suppressing the growth of the others until finally a single parallel-sided finger, whose nose shape is independent of time, has developed (Saffman and Taylor [9], Gupta *et al.* [5], Pitts [8]). Similar behaviour has been observed in a bead-packed porous medium model (Gupta and Greenkorn [6]). Although the steady finger remains stable over a large range of speeds, Saffman and Taylor [9] report that, at very high speeds, it divides into smaller fingers.

Conditions governing the onset of instability from an initially plane interface have been derived by Saffman and Taylor [9] and Chouke *et al.* [2] and include viscous, gravitational and interfacial parameters. Saffman and Taylor [9] describe solutions for the profiles of fully developed fingers of arbitrary width when interfacial tension is ignored and Saffman [10] gives similar solutions for the growth of fingers from an approximately sinusoidal perturbation of a flat interface. McLean and Saffman [7] derive fully developed finger shapes, which include interfacial tension effects, as numerical solutions of a nonlinear integro-differential equation.

De Josselin de Jong [3] describes an approach in which the two different fluids are replaced by a single hypothetical fluid with vortices along the interface to account for the change in fluid properties. Attention was focused on the case of fluids with equal viscosity but different density in the absence of interfacial tension; however it was noted that vortex strength must depend on the unknown solution to account for viscosity differences. This suggests a Green's function approach to the general problem, culminating in an integral equation describing the flow.

In this paper an integral equation for the normal velocity of the interface, which includes interfacial tension, is derived in terms of the physical parameters, a Green's function and the given interface. The primary objective is to extend the theoretical basis for the modelling of unstable displacements.

2. The problem

Consider an infinitely long, thin vertical porous layer of width L (Figure 1) in which one fluid (density ρ_1, viscosity μ_1) is being displaced upwards by another (density ρ_2, viscosity μ_2). The interface (denoted by C) separating the two fluids

https://doi.org/10.1017/S0334270000004306 Published online by Cambridge University Press

is assumed to be sharp and the motion at large distances upstream and downstream of the interface is taken to be uniform with velocity V. The densities ρ_1 and ρ_2 are assumed to be constant.

The flow can be considered as two-dimensional for which Darcy's Law gives, for each fluid ($i = 1, 2$),

$$u_i = \frac{-k}{\mu_i}\frac{\partial p_i}{\partial x}, \qquad v_i = \frac{-k}{\mu_i}\left(\frac{\partial p_i}{\partial y} + \rho_i g\right), \tag{1}$$

and hence, from the continuity equation,

$$\nabla^2 p_i = 0 \tag{2}$$

where (x, y) are the usual rectangular coordinates with y being the upward vertical, k is the permeability, g is the acceleration due to gravity, p_i is the pressure and u_i, v_i are the velocity components in the x, y directions, respectively. The effect of immobile residual fluid can be incorporated simply by changing the mobility k/μ_i of each fluid in equations (1). Equations (1) also hold for flow between two closely spaced parallel plates (Hele-Shaw cell) where u_i, v_i now correspond to mean velocities over the spacing b and $k = b^2/12$.

At the interface, the normal velocity (u_n) is continuous, hence

$$u_n = \frac{-k}{\mu_1}\left(\frac{\partial p_1}{\partial n} + \rho_1 g\cos\theta\right) = \frac{-k}{\mu_2}\left(\frac{\partial p_2}{\partial n} + \rho_2 g\cos\theta\right) \tag{3}$$

on C where the normal n is directed from the lower to the upper fluid, and θ is the angle made between the normal and positive y axis.

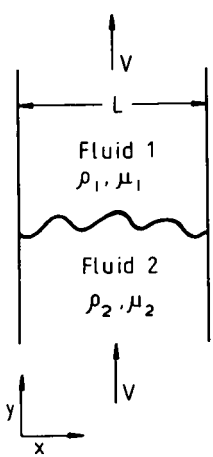

Figure 1. Schematic representation of the vertical displacement of fluid 1 (density ρ_1 and viscosity μ_1) by fluid 2 (density ρ_2 and viscosity μ_2) in a two-dimensional porous medium or Hele-Shaw cell of width L, the velocity at infinity being V.

https://doi.org/10.1017/S0334270000004306 Published online by Cambridge University Press

In general, there is also a jump in the pressure at the interface the magnitude of which depends, at the microscopic level, on the interfacial tension (γ), microscopic curvature and the normal viscous stress. The latter is usually ignored when pore-to-pore variations are smoothed out (it can also be ignored on a pore scale when $\mu V/\gamma \ll 1$ [13]) and it is commonly assumed that the pressure jump across the macroscopic interface C is given by

$$p_2 - p_1 = \gamma H(x, y) + P_c \tag{4}$$

where γ is now an effective interfacial tension which may be much larger than the ordinary bulk interfacial tension, H is the macroscopic curvature of the interface and P_c is a constant 'capillary' pressure associated with the microscopic interfaces underlying C. Physically, P_c is much greater than the pressure difference due to the macroscopic curvature H; however the term γH cannot then be ignored since the flow is independent of a constant P_c, regardless of its magnitude.

Condition (4), with γ taken to be the bulk interfacial tension, has also been proposed at the interface in a Hele-Shaw cell (Saffman and Taylor [9], Chuoke *et al.* [2]) where, for example, P_c is replaced by $2\gamma/b$ corresponding to a uniform semi-circular meniscus between the plates of the cell. Other choices of P_c take account of a non-zero contact angle (assumed constant) and the presence of a uniform film of displaced fluid remaining on the plates. Although the choice of constant P_c is probably a good approximation in Hele-Shaw cells for small deviations from a horizontal interface, recent evidence (Pitts [8], McLean and Saffman [7]) suggests that, in general, the curvature of the meniscus varies along the interface, corresponding to variations in film thickness. Theoretical [1] and experimental [4, 12] studies of a finger of negligible viscosity, moving steadily with velocity U in a tube, found that film thickness depends on $\mu U/\gamma$; a similar dependence is expected at each point of the interface C in a Hele-Shaw cell with U replaced by u_n. (When $\mu U/\gamma \ll 1$, viscous stresses significantly affect the steady, profile shape only near the walls of the tube and Bretherton [1] has applied the lubrication hypothesis in this region.) However, a proper determination of the pressure drop across C appears to require an analysis of the three-dimensional flow near the interface.

For a uniform velocity V at infinity, we require (using equation (1))

$$\begin{aligned} p_1 &\to -K_1 y + A_1 \quad \text{as } y \to \infty, \\ p_2 &\to -K_2 y + A_2 \quad \text{as } y \to -\infty, \end{aligned} \tag{5}$$

where $K_i = \mu_i V/k + \rho_i g$ and A_1, A_2 are arbitrary functions of x. At the side walls, we require $u_i = 0$, hence

$$\partial p_i/\partial x = 0 \quad \text{for } x = 0 \text{ and } x = L. \tag{6}$$

The objective is to use a Green's function for the problem to obtain a boundary integral representation for u_n.

https://doi.org/10.1017/S0334270000004306 Published online by Cambridge University Press

3. The Green's function

A function $G(x, y; \zeta, \eta)$ satisfying

$$\nabla^2 G = \delta(x-\zeta)\delta(y-\eta) \tag{7}$$

in the region $0 < x, \zeta < L$, $-\infty < y, \eta < \infty$, together with the side wall boundary condition (6), is given by

$$G(x, y; \zeta, \eta) = \frac{1}{4\pi}\left(\log\left(\cosh\frac{\pi}{L}(y-\eta) - \cos\frac{\pi}{L}(x+\zeta)\right)\right.$$
$$\left. + \log\left(\cosh\frac{\pi}{L}(y-\eta) - \cos\frac{\pi}{L}(x-\zeta)\right)\right) \tag{8}$$

where

$$G \to \frac{1}{2L}|y-\eta| - \frac{1}{2\pi}\log 2, \qquad |y-\eta| \to \infty;$$
$$G \to E(x, y; \zeta, \eta) \quad \text{for } (\zeta, \eta) \to (x, y) \text{ and } 0 < x < L,$$

and

$$G \to 2E(x, y; 0, \eta) \quad \text{for } \zeta \to 0,$$
$$\to 2E(x, y; L, \eta) \quad \text{for } \zeta \to L,$$

where

$$E = \frac{1}{2\pi}\log r \quad \text{and} \quad r^2 = (y-\eta)^2 + (x-\zeta)^2.$$

Hereafter, we use an abbreviated notation, writing $G(X; \xi)$, $E(X; \xi)$ where X and ξ are the points (x, y) and (ζ, η), respectively.

4. The integral equation

Consider the Green's theorem

$$\int_R \left(p\nabla^2 G - G\nabla^2 p\right) d\xi = \int_{\partial R}\left(p\frac{\partial G}{\partial N} - G\frac{\partial p}{\partial N}\right) dS$$

where ∂R is the boundary of region R, N is the outward normal to ∂R and S is arc length. If point $X = (x, y)$ lies within the upper fluid (R_1), then applying Green's theorem over regions R_1 and R_2 in turn, and adding the resulting expressions gives

$$p_1(X) = \text{constant} - \tfrac{1}{2}(K_1 + K_2)y + \int_C \left(p_2(\xi) - p_1(\xi)\right)\frac{\partial G(X; \xi)}{\partial n(\xi)} dS(\xi)$$
$$- \int_C \left(\frac{\partial p_2}{\partial n} - \frac{\partial p_1}{\partial n}\right) G(X; \xi)\, dS(\xi) \tag{9}$$

https://doi.org/10.1017/S0334270000004306 Published online by Cambridge University Press

(note that $N = -n$ when $R = R_1$ and $N = n$ when $R = R_2$). The same procedure results in an identical expression for $p_2(X)$ when X lies within the lower fluid (R_2). By substituting the interface conditions (3) and (4) into expression (9) we get

$$p_1(X) = \text{constant} - \tfrac{1}{2}(K_1 + K_2)y + \gamma \int_C H(\xi) \frac{\partial G(X;\xi)}{\partial n(\xi)} dS(\xi) - \int_C \left(\frac{1}{k}(\mu_1 - \mu_2)u_n(\xi) + (\rho_1 - \rho_2)g\cos\theta \right) G(X;\xi)\, dS(\xi), \quad (10)$$

and an expression of the same form for $p_2(X)$. Note that equation (A7) shows that the integral involving capillary pressure P_c is a constant. This is expected since, initially, we could have set $P_c = 0$ simply by adding constants to p_1 and p_2.

The determination of u_n on C is of fundamental interest, not only because it describes the motion of the interface, but also because the pressure at any point can then be calculated from equation (10). Limiting expressions for $\partial p_1/\partial n$ and $\partial p_2/\partial n$ as X approaches C from above and below, respectively, may be derived from equation (10) by using results (A1) and (A3). By adding these expressions and using the interface condition (3), we find that

$$u_n(X) = V\cos\theta(X) + 2\int_C F(\xi) \frac{\partial G(X;\xi)}{\partial n(X)} dS(\xi) - \frac{2\gamma k}{\mu_1 + \mu_2} \left(\int_C M(X;\xi)\, dS(\xi) - \frac{dH(X)}{dS}(G(X;\xi_L) - G(X;\xi_0)) \right) \quad (11)$$

for $0 < x < L$ on C, where

$$F(\xi) = \left(\frac{\mu_1 - \mu_2}{\mu_1 + \mu_2} \right) u_n(\xi) + kg \left(\frac{\rho_1 - \rho_2}{\mu_1 + \mu_2} \right) \cos\theta(\xi),$$

and

$$M(X;\xi) = (H(\xi) - H(X)) \frac{\partial^2 G}{\partial n(X)\partial n(\xi)} + \frac{dH(X)}{dS} \frac{\partial G}{\partial S(\xi)}.$$

By taking the derivative of equation (4) along the curve C, evaluating it at the end points of C, and using equations (1) and (6), we get

$$\gamma \frac{dH}{dS}\cos\theta = \left((\rho_1 - \rho_2)g\cos\theta + \frac{1}{k}(\mu_1 - \mu_2)u_n \right) \sin\theta \quad (12)$$

at $x = 0$ and $x = L$. Thus, condition (A6) is satisfied with respect to the two integrals in equation (10), and $\partial p_1/\partial n + \partial p_2/\partial n$ may be evaluated at the end points of C, as required. Results (A5) and (12) can be applied to equation (10) to

https://doi.org/10.1017/S0334270000004306 Published online by Cambridge University Press

show that, when $x = 0$ or L,

$$u_n(X) = V\cos\theta + \frac{2j}{\pi}\left(\frac{\gamma k}{\mu_1 + \mu_2}\right)\frac{dH}{dS}(\theta\cot\theta - \cos^2\theta) + 2\int_C D(X;\xi)\,dS(\xi) \tag{13}$$

where

$$D(X;\xi) = F(\xi)\frac{\partial G}{\partial n(X)} - \frac{\gamma k}{\mu_1 + \mu_2}(H(\xi) - H(X))\frac{\partial^2 G}{\partial n(X)\partial n(\xi)},$$

and

$$j = \begin{cases} 1, & x = 0, \\ -1, & x = L. \end{cases}$$

Note that the integrands in equations (11) and (13) are finite when $\xi = X$ since the singular parts of the corresponding component terms cancel.

We consider the following points:

(i) When $\theta = 0$ at an end point, equation (12) shows that either $\gamma = 0$ or $dH/dS = 0$ there. That is, when the interface is normal to a side wall, it also has a local maximum or minimum of curvature there, unless the interfacial tension is zero. In this case, the integral equations (11) and (13) are equivalent, the latter then applying at this end point as well as at interior points of C.

(ii) When $\theta = \pm\frac{1}{2}\pi$ at an end point, $u_n = 0$.

(iii) Equations (12) and (13) place constraints on the behaviour of the interface at its end points for given physical parameters. However, there seems to be no straightforward and general way of determining such behaviour at end points with $\theta \neq 0, \pm\frac{1}{2}\pi$ when $\mu_1 \neq \mu_2$; we therefore confine ourselves to the above cases (i) and (ii) in the examples to follow (Section 6).

(iv) When $\mu_1 = \mu_2$, $u_n(\xi)$ disappears from the integrands in equations (11) and (13), so $u_n(X)$ is expressed as an integral of known quantities.

(v) In the special case of no flow, equations (1) and (4) show that

$$\gamma\frac{dH}{dS} = (\rho_1 - \rho_2)g\sin\theta,$$

and hence

$$\gamma H = (\rho_1 - \rho_2)g\eta + \text{constant},$$

at all points on C. This corresponds to the balance between gravitational force and interfacial tension. That the integral equation is satisfied may be confirmed by comparison with results (A10) and (A11).

https://doi.org/10.1017/S0334270000004306 Published online by Cambridge University Press

5. Comparison with steady solutions

Consider the steady advance of a single, parallel sided finger of displacing fluid in which the nose section (C_1) moves forward with velocity V_1^* and the tail section (C_2) moves backward with velocity V_2^*. In Figure 2, C_1 is the curve AOF and C_2 consists of the two curves BC and ED. The parallel vertical sections AB and EF have length $\gg 1$ and are denoted by C_3. When $\gamma = 0$, curve C_1 is given by the Saffman-Taylor solution which, for a finger of width 2λ in a cell of width $L = 2$, is

$$y^* = \frac{2}{\pi}(1-\lambda)\log\cos\frac{\pi x^*}{2\lambda} \tag{14}$$

where (x^*, y^*) are coordinates with respect to an origin 0 located at the nose of the finger.

Now, by equation (1), $\partial p_1/\partial y = \mu_1 V_2^*/k - \rho_1 g$, on C_2 and, $\partial p_2/\partial y = -\mu_2 V_1^*/k - \rho_2 g$, on C_1. However, we see from condition (4) that $\partial p_1/\partial y = \partial p_2/\partial y$ on the vertical sections C_3 which match C_1 and C_2 (this remains true when $\gamma \neq 0$ since C_3 has zero curvature). Thus

$$\mu_2 V_1^* + \mu_1 V_2^* = kg(\rho_1 - \rho_2). \tag{15}$$

Conservation of mass is given by

$$\int_C u_n(X)\, dS(X) = VL, \tag{16}$$

and hence

$$V = \lambda V_1^* - (1-\lambda)V_2^*. \tag{17}$$

Both expressions (15) and (17) have been derived previously by Saffman and Taylor [9].

Now, for X lying on C_1,

$$\int_{C_1} F(\xi)\partial G/\partial n(X)\, dS(\xi) = \frac{(\mu_1-\mu_2)V_1^* + kg(\rho_1-\rho_2)}{\mu_1+\mu_2} \cdot \int_{C_1} \cos\theta(\xi)\partial G/\partial n(X)\, dS(\xi)$$

and, since $\partial G/\partial n(X) \to \frac{1}{4}\cos\theta(X)$ when $L = 2$ as $\eta \to -\infty$,

$$\int_{C_2} F(\xi)\partial G/\partial n(X)\, dS(\xi) = \frac{1}{2}(1-\lambda)\frac{(-(\mu_1-\mu_2)V_2^* + kg(\rho_1-\rho_2))}{\mu_1+\mu_2}\cos\theta(X)$$

where

$$u_n = \begin{cases} V_1^*\cos\theta & \text{on } C_1, \\ -V_2^*\cos\theta & \text{on } C_2. \end{cases}$$

https://doi.org/10.1017/S0334270000004306 Published online by Cambridge University Press

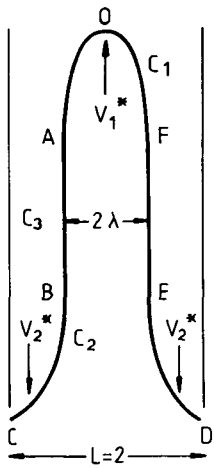

Figure 2. Schematic representation of a single, steadily advancing, parallel sided finger of width 2λ in a medium of width $L = 2$. The finger nose AOF (denoted by C_1) is advancing with velocity V_1^* and the tail sections BC and ED (denoted by C_2) are retreating with velocity V_2^*. C_3 refers to the vertical sections AB and EF which match C_1 and C_2.

On C_3, $F = 0$ (as $u_n = \cos\theta = 0$) and the corresponding integral is zero. Thus, by using expressions (15) and (17) in equation (11) for $\gamma = 0$, we can show that the Saffman-Taylor profile (equation (14)) must satisfy

$$\int_{C_1} \cos\theta(\xi)\partial G/\partial n(X)\, dS(\xi) = \tfrac{1}{2}(1-\lambda)\cos\theta(X)$$

for all X on C_1, a result which may be demonstrated to a high degree of accuracy by numerical integration. Similarly, when $\gamma \neq 0$, we can show that the finger C_1 must satisfy

$$\int_{C_1}\left(\cos\theta(\xi)\frac{\partial G}{\partial n(X)} - \frac{\gamma k}{\mu_1(V_1^* + V_2^*)}M(X;\xi)\right) dS(\xi) = \tfrac{1}{2}(1-\lambda)\cos\theta(X) \tag{18}$$

for all X on C_1.

McLean and Saffman [7] have derived fully developed finger shapes corresponding to curve C_1, which include interfacial tension effects, as numerical solutions of a nonlinear, integro-differential equation (gravity was ignored and the displacing fluid was assumed to have negligible viscosity μ_2). These shapes, together with the corresponding relationship between λ and $\gamma k/(\mu_1 V_1^*)$ (derived by McLean and Saffman as part of their solution), must satisfy equation (18); however, it is not convenient to confirm this directly, as the McLean-Saffman curves can only be derived numerically. Instead, for these curves, we use an approximate analytical form which was noted by Pitts [8] and is given by equation (14) with the multiplier $(1-\lambda)$ replaced by λ. Using McLean and

https://doi.org/10.1017/S0334270000004306 Published online by Cambridge University Press

Saffman's data relating λ to $\gamma k/(\mu_1 V_1^*)$ ([7], Table 1 and equation (17)), we find that equation (18) is satisfied with an error which increases with λ (see Table 1, this paper), corresponding to the apparent increasing deviation between the Pitts approximating curves and the McLean-Saffman exact curves.

TABLE 1. Maximum error in equation (18) when fully developed fingers in the case $\mu_2 = 0$, $g = 0$ are represented by the Pitts approximate analytical form and the relationship between λ and $\gamma k/(\mu_1 V_1^*)$ is given by the McLean-Saffman calculations.

λ	Maximum Error		λ	Maximum Error
0.515	0.0044		0.678	0.0282
0.524	0.0062		0.720	0.0390
0.537	0.0075		0.767	0.0594
0.557	0.0096		0.809	0.0836
0.582	0.0125		0.881	0.1407
0.604	0.0158		0.947	0.2377
0.640	0.0242		0.984	0.3743

6. Numerical solutions

The integral equation (11) can be solved numerically by standard methods (quadrature of the integral followed by collocation to obtain a set of simultaneous linear algebraic equations). However, unless $\theta = 0$ at both ends of C, it is first necessary that $F(\xi)\partial G/\partial n(X)$ in equation (11) be replaced by $F(\xi)\partial G/\partial n(X) - F(X)\partial G/\partial n(\xi)$ (this is permissible by equation (A8)) to ensure accuracy. This becomes clearer if we consider equation (B1). At interior points X of C, $(\partial G/\partial n(X))_{\xi=X}$ increases in magnitude as $x \to 0$ or L (unless $\theta \to 0$ also) and will magnify numerical errors in u_n near the side walls. However, this effect may be substracted, as is indicated above. A useful check on the numerical procedure is the conservation of mass requirement (equation (16)).

Attention is focused on cases (i) and (ii) in Section (4) for which $\theta = 0$ or $\theta = \pm \frac{1}{2}\pi$, so that condition (12) is satisfied independently of γ. In these cases it is convenient to separate out the effect of interfacial tension by setting

$$u_n(X) = W_1(X) + \alpha_2 W_2(X),$$

so that

$$W_2(X) = 2\alpha_1 \int_C W_2(\xi)\partial G/\partial n(X)\, dS(\xi) - 2L^2 V\left(\int_C M(X;\xi)\, dS(\xi) - \frac{dH(X)}{dS}(G(X;\xi_L) - G(X;\xi_0))\right), \tag{19}$$

https://doi.org/10.1017/S0334270000004306 Published online by Cambridge University Press

by equation (11), where $\alpha_1 = (\mu_1 - \mu_2)/(\mu_1 + \mu_2)$ and $\alpha_2 = \gamma k/(L^2 V(\mu_1 + \mu_2))$ are dimensionless parameters, W_1 is the normal velocity of C when $\gamma = 0$ and W_2 is a function describing the pattern of the correction, due to interfacial tension, to the normal velocity.

To illustrate, we assume that $V = L = 1$ and $\rho_1 = \rho_2$, and normal velocities W_1 and W_2 are calculated for two different interfaces given by

(a)

$$y = \left(\frac{1}{4} - \left(x - \frac{1}{2}\right)^2\right)^{\frac{1}{2}} \quad (i.e.\ \text{a semicircle}),$$

and

(b)

$$y = \cos \pi x,$$

and the results are plotted in Figures 3 and 4. In case (a), curvature is constant, so $W_2(X) = 0$ and $u_n(X) = W_1(X)$. In case (b), $\theta = 0$ at the side walls, so $du_n/dx = 0$ there (since $u_i = 0$ on the side walls and $\partial u_i/\partial y = \partial v_i/\partial x$).

When $\mu_1 = \mu_2$ (i.e. $\alpha_1 = 0$), $W_1 = \cos\theta$ corresponding to uniform flow everywhere of a single, homogeneous fluid. When the upper fluid is much more viscous

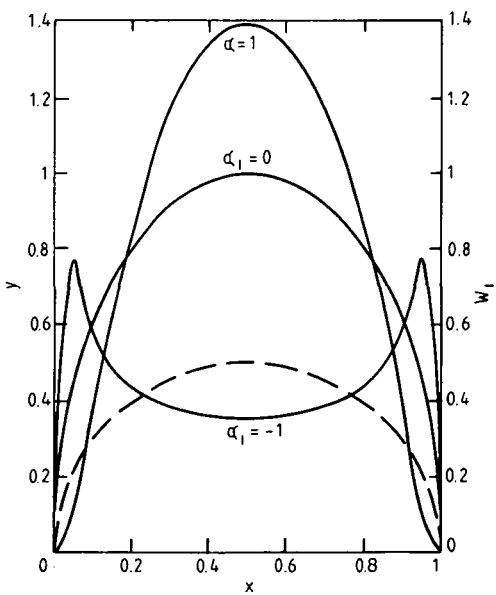

Figure 3. Normal velocity W_1 (solid curves) of a semicircular interface (dashed curve) plotted against x for different values of the parameter $\alpha_1 = (\mu_1 - \mu_2)/(\mu_1 + \mu_2)$.

https://doi.org/10.1017/S0334270000004306 Published online by Cambridge University Press

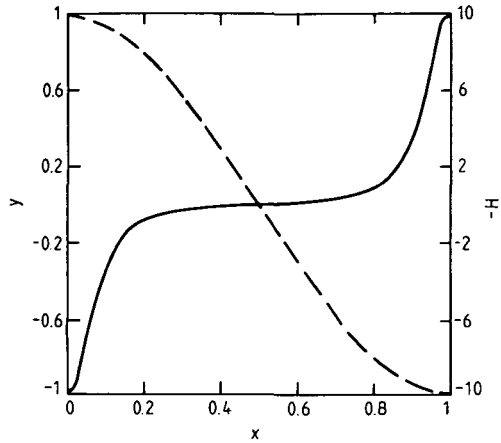

Figure 4(a). An interface $y = \cos \pi x$ (dashed curve) with curvature H. The solid curve is a plot of $-H$ against x.

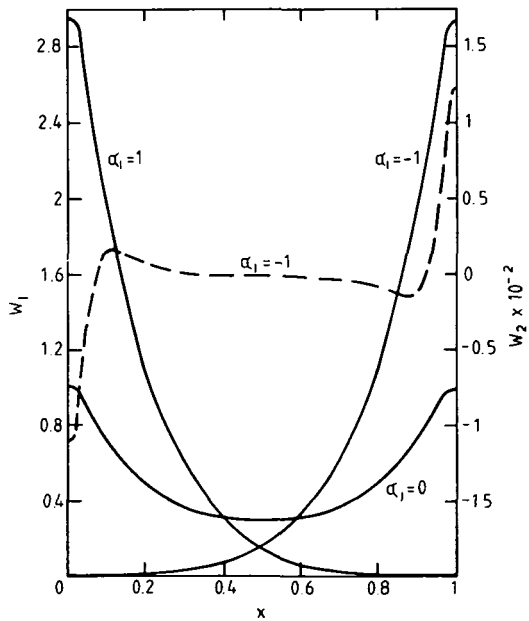

Figure 4(b). Normal velocity (W_1) in the absence of interfacial tension (γ) of the above interface is plotted (solid curves) against x for different values of the parameter $\alpha_1 = (\mu_1 - \mu_2)/(\mu_1 + \mu_2)$. The component of the normal velocity due to interfacial tension is $\alpha_2 W$ where $\alpha_2 = \gamma k/(L^2 V(\mu_1 + \mu_2))$. The dashed curve is a plot of W_2 against x for $\alpha_1 = -1$ (the curve for $\alpha_1 = 1$ is very similar).

https://doi.org/10.1017/S0334270000004306 Published online by Cambridge University Press

than the lower, displacing fluid (i.e. $\alpha_1 = 1$), W_1 in Figures 3 and 4 is greater or less than that for uniform flow near points of maximum or minimum displacement of fluid 1 by fluid 2. The interface will therefore tend to increase in amplitude. Conversely, when the upper fluid is much less viscous than the lower (i.e. $\alpha_1 = -1$), the opposite is true and the amplitude tends to decrease. This is consistent with conclusions about stability based on an analysis of small perturbations of a horizontal interface under the same conditions. Saffman and Taylor [9] and Chuoke *et al.* [2] showed that small perturbations of the form

$$y = \varepsilon \exp(inx + \sigma t),$$

satisfy

$$(\mu_1 + \mu_2)\sigma/n = (\mu_1 - \mu_2)V + kg(\rho_1 - \rho_2) - n^2\gamma k, \tag{20}$$

and the disturbance is unstable when $\sigma > 0$ and stable when $\sigma < 0$. In particular, when $\rho_1 = \rho_2$ and $\gamma = 0$, $\sigma \gtrless 0$ when $\alpha_1 \gtrless 0$.

The contribution $(\alpha_2 W_2)$ to u_n made by interfacial tension depends on curvature and is more complicated than W_1. In Figure 4(b), W_2 is plotted for $\alpha_1 = -1$ (in this case little difference is found between the W_2 curves corresponding to $\alpha_1 = \pm 1$). In the central part, curvature (H) is low, hence W_2 is small. Near $x = 0$, H (and $p_2 - p_1$ on C) becomes large and positive and local pressure gradients become less negative, decreasing u_n and hence W_2, as is shown in Figure 4(b). Conversely, near $x = 1$, H becomes large and negative, u_n and hence W_2 must increase. Thus interfacial tension appears to hasten amplitude reduction during stable flows and slow amplitude growth during unstable flows, a result consistent with equation (20).

7. Conclusion

In summary, we have presented an integral equation for the velocity of the interface between two immiscible viscous fluids in a two-dimensional porous medium or Hele-Shaw cell when one of the fluids is displaced by the other. Knowledge of this velocity permits the evaluation of the pressure at any point. It is also necessary for a stepwise determination of the evolution of the interface and, at each step, consideration of an integral equation is preferable to a numerical solution for flow over the whole fluid region.

The Saffman-Taylor profiles are seen to satisfy the integral equation when $\gamma = 0$. Similarly, when $\gamma \neq 0$, it is shown that the Pitts approximating profiles, together with the McLean-Saffman data relating finger width to interfacial tension, satisfy the integral equation with an error which increases with λ, corresponding to the increasing error between the Pitts approximating function and the exact profile.

Appendix A

Some integral properties on C

Let

$$f(X) = \int_C a(\xi)G(X;\xi)\,dS(\xi),$$

and

$$h(X) = \int_C b(\xi)\frac{\partial G(X;\xi)}{\partial n(\xi)}dS(\xi),$$

where S is the arc length along curve C. If $G(X;\xi)$ is replaced by $E(X;\xi)$ then f and h define a simple layer and a double layer, respectively. Using standard techniques (Stakgold [11], page 121) one can show that
(i) For $0 < x_0 < L$

$$\lim_{X\to X_0\pm} \partial f(X)/\partial\nu = \pm\frac{1}{2}a(X_0) + \int_C a(\xi)\frac{\partial G(X_0;\xi)}{\partial n(X_0)}dS(\xi), \tag{A1}$$

$$\lim_{X\to X_0\pm} h(X) = \mp\frac{1}{2}b(X_0) + \int_C b(\xi)\frac{\partial G(X_0;\xi)}{\partial n(\xi)}dS(\xi), \tag{A2}$$

$$\lim_{X\to X_0\pm} \partial h(X)/\partial\nu$$

$$= \int_C \left((b(\xi) - b(X_0))\frac{\partial^2 G}{\partial n(X_0)\partial n(\xi)} + \frac{db(X_0)}{dS}\frac{\partial G}{\partial S(\xi)} \right) dS(\xi)$$

$$- \frac{db(X_0)}{dS}(G(X_0;\xi_L) - G(X_0;\xi_0)), \tag{A3}$$

where $\xi_0 = (0,\eta)$ and $\xi_L = (L,\eta)$, ν is the upward normal direction $n(X_0)$ as $X \to X_0$ on C and plus or minus indicates that the limit in X is taken from above or below C, respectively. The method involves splitting C into two parts, $C - C_\varepsilon$ and C_ε where C_ε is a small segment containing the point X_0, then taking the limit $\varepsilon \to 0$ after the limit in X. For $\lim_{X\to X_0\pm} \partial h(X)/\partial\nu$ one first obtains

$$\int_C \left(b(\xi)\frac{\partial^2 G}{\partial n(X_0)\partial n(\xi)} - b(\xi)\frac{\partial^2 G}{\partial S^2(\xi)} + \frac{d^2 b(\xi)}{dS^2}G \right) dS(\xi)$$

$$+ \left(b\frac{\partial G}{\partial S(\xi)} - \frac{db}{dS}G \right)_{\xi_0}^{\xi_L}.$$

https://doi.org/10.1017/S0334270000004306 Published online by Cambridge University Press

Equation (A3) is then derived by integration by parts after recognising that

$$\int_C \left(\frac{\partial^2 G}{\partial n(X_0)\partial n(\xi)} - \frac{\partial^2 G}{\partial S^2(\xi)} \right) dS(\xi) + \left(\frac{\partial G}{\partial S(\xi)} \right)_{\xi_0}^{\xi_L} = 0$$

(set $b = 1$ and use result (A7)) and that

$$(b(\xi) - b(X_0)) \frac{\partial G}{\partial S(\xi)} \quad \text{and} \quad \left(\frac{db(\xi)}{dS} - \frac{db(X_0)}{dS} \right) G(X_0; \xi),$$

are finite at $\xi = X_0$.

(ii) For $x_0 = 0$ or $x_0 = L$

$$\lim_{X \to X_0 \pm} h(X) = \left(\mp \frac{1}{2} - \frac{j\theta}{\pi} \right) b(X_0) + \int_C b(\xi) \frac{G(X_0; \xi)}{\partial n(\xi)} dS(\xi), \tag{A4}$$

where

$$j = \begin{cases} 1, & x_0 = 0, \\ -1, & x_0 = L. \end{cases}$$

When X_0 is an end point of C, equations (A1–A3) still apply, provided C is normal to the side wall (i.e. $\theta(X_0) = 0$). Equations (A1) and (A3) also hold at an end point when $a(X_0) = 0$ and $db(X_0)/dS = 0$, respectively. When $\theta(X_0) = \pm \frac{1}{2}\pi$, $\partial f/\partial \nu$ and $\partial h/\partial \nu \to 0$ as $X \to X_0 \pm$. In general,

$$\begin{aligned} \lim_{X \to X_0 \pm} & (\partial f/\partial \nu + \partial h/\partial \nu) \\ &= \left(\pm \frac{1}{2} + \frac{j\theta}{\pi} \right) a(X_0) + \frac{j}{\pi} \cos^2 \theta \frac{db}{dS}(X_0) \\ &\quad + \int_C \left(a(\xi) \frac{\partial G}{\partial n(X_0)} + (b(\xi) - b(X_0)) \frac{\partial^2 G}{\partial n(X_0)\partial n(\xi)} \right) dS(\xi), \end{aligned} \tag{A5}$$

provided

$$db/dS \cos \theta + a \sin \theta = 0 \quad \text{when } X = X_0. \tag{A6}$$

(iii) Additional results

$$\int_C \frac{\partial G(X; \xi)}{\partial n(\xi)} dS(\xi) = \begin{cases} -\frac{1}{2} & \text{if } X \in R_1, \\ \frac{1}{2} & \text{if } X \in R_2. \end{cases} \tag{A7}$$

and

$$\int_C \frac{\partial G(X_0; \xi)}{\partial n(\xi)} dS(\xi) = \frac{j\theta}{\pi}, \tag{A8}$$

https://doi.org/10.1017/S0334270000004306 Published online by Cambridge University Press

for points X_0 lying on C and setting $j = 0$ when $0 < x_0 < L$. Also

$$\int_C \left(\cos\theta(\xi) G(X;\xi) - \eta \frac{\partial G(X;\xi)}{\partial n(\xi)} \right) dS(\xi) = \begin{cases} \frac{1}{2} y - \frac{L}{2\pi} \log 2 & \text{if } X \in R_1, \\ -\frac{1}{2} y - \frac{L}{2\pi} \log 2 & \text{if } X \in R_2. \end{cases} \tag{A9}$$

Hence

$$\int_C \left(\cos\theta(\xi) \frac{\partial G}{\partial n(X_0)} - (\eta - y) \frac{\partial^2 G}{\partial n(X_0) \partial n(\xi)} - \sin\theta(X_0) \frac{\partial G}{\partial S(\xi)} \right) dS(\xi) + \sin\theta(X_0)(G(X_0;\xi_L) - G(X_0;\xi_0)) = 0 \tag{A10}$$

for $X_0 \in C$ and $0 < x_0 < L$, and

$$\int_C \left(\cos\theta(\xi) \frac{\partial G}{\partial n(X_0)} - (\eta - y) \frac{\partial^2 G}{\partial n(X_0) \partial n(\xi)} \right) dS(\xi) + \frac{j}{\pi} \cos\theta(\theta - \sin\theta\cos\theta) = 0, \tag{A11}$$

for $X_0 \in C$ and $x_0 = 0$ or L using results (A1), (A3) and (A5).

Appendix B

Integrand values when $\xi = X$

The integrands in equations (11) and (13) are continuous in ξ for given X. In the following we give the values of those integrands at the point $\xi = X$. The curvature of the interface is denoted here by $K(X)$; $H(X)$ in equation (4) is now presumed to be a general function (in the main text it is assumed that $H = K$).

(a) $0 < x < L$

$$\frac{\partial G}{\partial n(X)} = \frac{K}{4\pi} - \frac{\sin\theta}{4L} \cot\frac{\pi x}{L}, \tag{B1}$$

$$M(X;X) = \frac{1}{4L} \frac{dH}{dS} \cos\theta \cot\frac{\pi x}{L} - \frac{1}{4\pi} \frac{d^2 H}{dS^2}. \tag{B2}$$

https://doi.org/10.1017/S0334270000004306 Published online by Cambridge University Press

(b) $x = 0, L; \theta = 0$

$$\frac{\partial G}{\partial n(X)} = \frac{K}{2\pi}, \tag{B3}$$

$$M(X; X) = -\frac{1}{2\pi}\frac{d^2H}{dS^2}. \tag{B4}$$

Note that $dH/dS = 0$ in this case.

(c) $x = 0, L$; **all** θ

$$D(X; X) = \frac{1}{2\pi}\left(\frac{\gamma k}{\mu_1 + \mu_2}\cos^2\theta\frac{d^2H}{dS^2} + KF\cos^2\theta - \sin 2\theta\frac{dF}{dS}\right) \tag{B5}$$

where

$$F = \left(\frac{\mu_1 - \mu_2}{\mu_1 + \mu_2}\right)u_n + k\left(\frac{\rho_1 - \rho_2}{\mu_1 + \mu_2}\right)g\cos\theta.$$

References

[1] F. P. Bretherton, "The motion of long bubbles in tubes", *J. Fluid Mech.* 10 (1961), 166–188.

[2] R. L. Chuoke, P. van Meurs and C. van der Poel, "The instability of slow, immiscible, viscous liquid-liquid displacements in permeable media", *Trans. AIME* 216 (1959), 188–194.

[3] G. de Josselin de Jong, "Singularity distributions for the analysis of multiple-fluid flow through porous media", *J. Geophys. Res.* 65 (1960), 3739–3758.

[4] F. Fairbrother and A. E. Stubbs, "The 'bubble-tube' method of measurement", *J. Chem. Soc.* 1 (1935), 527–529.

[5] S. P. Gupta, J. E. Varnon and R. A. Greenkorn, "Viscous finger wavelength degeneration in Hele-Shaw models", *Water Resources Res.* 9 (1973), 1039–1046.

[6] S. P. Gupta and R. A. Greenkorn, "An experimental study of immiscible displacement with an unfavourable mobility ratio in porous media", *Water Resources Res.* 10 (1974), 371–374.

[7] J. W. McLean and P. G. Saffman, "The effect of surface tension on the shape of fingers in a Hele-Shaw cell", *J. Fluid Mech.* 102 (1981), 455–469.

[8] E. Pitts, "Penetration of fluid into a Hele-Shaw cell: the Saffman-Taylor experiment", *J. Fluid Mech.* 97 (1980), 53–64.

[9] P. G. Saffman and Sir Geoffrey Taylor, "The penetration of a fluid into a porous medium or Hele-Shaw cell containing a more viscous liquid", *Proc. Roy. Soc. London Ser. A* 245 (1958), 312–329.

[10] P. G. Saffman, "Exact solutions for the growth of fingers from a flat interface between two fluids in a porous medium or Hele-Shaw cell", *Quart. J. Mech. Appl. Math.* 12 (1959), 146–150.

[11] I. Stakgold, *Boundary value problems of mathematical physics*, Vol. II (Macmillan, New York, 1968).

[12] G. I. Taylor, "Deposition of a viscous fluid on the wall of a tube", *J. Fluid. Mech.* 10 (1961), 161–165.

[13] R. A. Wooding and H. J. Morel-Seytoux, "Multiphase fluid flow through porous media", *Ann. Rev. Fluid Mech.* 8 (1976), 233–274.